

Synthesis and sintering improvement of Aurivillius type structure ferroelectric ceramics by mechanochemical activation

Alicia Castro,* Pilar Millán, Lorena Pardo and Basilio Jiménez

Instituto de Ciencia de Materiales de Madrid, C.S.I.C. Cantoblanco, 28049 Madrid, Spain.
E-mail: acastro@icmm.csic.es

Received 29th March 1999, Accepted 8th April 1999

An oxide mixture of composition $3\text{Bi}_2\text{O}_3 : \text{Nb}_2\text{O}_5 : 2\text{TiO}_2$ has been mechanochemically activated in a laboratory mill for different times from 3 to 336 h. The as-milled powder and an unmilled mixture of identical composition were annealed at different temperatures up to the formation of the Aurivillius-type oxide $\text{Bi}_3\text{NbTiO}_9$, and examined by X-ray diffraction (XRD) and differential thermal analysis (DTA). The sample milled for 336 h shows complete amorphization. Its DTA curve exhibits two exothermic process at 370 and 560 °C, corresponding to the formation of a metastable fluorite phase and the Aurivillius-type oxide, respectively. The crystallization temperature of this Aurivillius phase from the unmilled oxide mixture is reported to be 1050 °C, whereas from the amorphous powder obtained by 336 h of mechanochemical activation this temperature becomes as low as 600 °C. Ceramics of this composition must be prepared by hot-pressing in order to obtain low porosities, owing to the lamellar morphology of the conventionally crystallized powder, which gives rise to textured anisotropic materials. Non-textured ceramics were obtained both from the conventionally crystallized and the amorphous powder by natural sintering at 1100 °C. Ceramics obtained from amorphous powder show lower porosity and higher electromechanical coupling factors.

Introduction

Aurivillius oxides are a family of materials built up by the stacking of $[\text{A}_{n-1}\text{B}_n\text{O}_{3n+1}]$ perovskite-like layers and bismuth–oxygen $[\text{Bi}_2\text{O}_2]$ slabs.¹ These compounds have received increasing interest as piezoelectric ceramic materials for use at high temperature, since they are ferroelectrics with high Curie temperature, anisotropic characteristics and useful properties, when prepared as thin films, for non-volatile FRAM memory and electro-optic devices.^{2–9} $\text{Bi}_3\text{NbTiO}_9$ constitutes a very interesting example in this family, where A and B sites in the perovskite layer are occupied by Bi^{3+} and $\text{Nb}^{5+}/\text{Ti}^{4+}$, respectively, and shows one of the highest Curie temperatures *ca.* 930 °C.¹⁰ Its production by classical ceramic methods is problematic because high temperatures and long reaction times are needed, as for other members of the Aurivillius family. Therefore, alternative routes for the preparation of these ferroelectric ceramic materials are of great interest.

Mechanochemical activation of inorganic compound mixtures has been applied to obtain amorphous materials, nanocrystals and intermetallic compounds.¹¹ More recently, it has also been used for the synthesis of ceramic materials with perovskite, ilmenite or fluorite type structures,^{12–14} as well as to obtain superconductor oxides.^{15,16} Some studies have also been devoted to the use of this technique in the production of functional materials, with the practical consequences of improved physicochemical characteristics of the treated materials.^{17–19}

During the mechanical treatment, materials are comminuted, the size of crystallites reduced, the crystal structures damaged and in most cases, the mechanically activated materials become more reactive and capable of faster reaction.^{20,21} Classical solid state chemical reactions become possible by heating the starting oxide mixture to a given temperature, at which the free energy of the system is higher than the activation free energy barrier. However, in the case of ball milling the free energy required for the activation is also supplied mechanically into the powder by ball impacts and stored in the formation of structural defects and microstrains. Thus the so-activated particles become capable of providing this energy to the synthesis or to the stabilization of metastable phases.^{20–23}

For this reason, we have attempted to improve the reaction

protocol, decreasing the reaction temperatures and times of Aurivillius oxides by mechanochemical activation of the starting oxide mixture by ball milling. Here, we report the physicochemical characteristics of the oxide $\text{Bi}_3\text{NbTiO}_9$, as a function of the milling time.

In addition, ceramics were prepared by natural sintering both from conventionally crystallized and from amorphous powders, and their properties compared.

Experimental

Stoichiometric mixtures of analytical grade Bi_2O_3 , Nb_2O_5 and TiO_2 were homogenized in an agate mortar for 3 min by hand. Then, the samples (*ca.* 2 g), were placed in a stainless-steel pot with a 5 cm diameter steel ball and mechanochemically activated on a Fritsch vibrating mill, model Pulverisette 0. Finally the samples were annealed at increasing temperatures from 500 to 900 °C for times ranging between 3 and 12 h. For the sake of comparison, $\text{Bi}_3\text{NbTiO}_9$ was also prepared by solid state reaction, at increasing temperatures (in seven steps) from 500 to 1050 °C with annealing times of 12 h. The products were slowly cooled to room temperature in the furnace, weighed, reground, and examined by X-ray powder diffraction after each treatment.

The thermal behaviour of the milled samples was examined by differential thermal analysis (DTA) and thermogravimetric analysis (TG) up to 1100 °C on a Seiko 320 instrument in air, at a heating rate of 10 °C min⁻¹, using *ca.* 10 mg of sample for each run. Al_2O_3 was used as the reference material.

Powder X-ray diffraction patterns were performed at room temperature with a Siemens Kristalloflex 810 computer controlled diffractometer, and a D 501 goniometer provided with a 2 θ compensating slit and a graphite monochromator. Patterns were collected in the range $2\theta = 5\text{--}100^\circ$ with increments of $2\theta = 0.05^\circ$ and a counting time of 4 s per step; the goniometer being controlled by a DACO-MPV2 computer. To collect X-ray diffraction patterns at high temperature, an Anton Paar HTK10 attachment mounted on a Philips PW 1310 diffractometer was used in the range $2\theta = 5\text{--}70^\circ$ with increments of $2\theta = 0.02^\circ$ and counting time of 2 s per step. Each sample was deposited on a platinum sheet placed on a

tantalum strip, which acts as the heating element. The temperature was measured using a Pt–13% Rh Pt thermocouple welded onto the center of the platinum sheet. The temperature was increased at a rate of $10\text{ }^{\circ}\text{C min}^{-1}$ and stabilized for the measurements. Cu-K α ($\lambda = 1.5418\text{ \AA}$) radiation was used in all experiments.

Conventionally crystallized and amorphous powders were preformed by uniaxial pressing at 300 kg cm^{-2} as thin discs of *ca.* 10 mm diameter and 2 mm thickness. Discs were isostatically pressed at 2000 kg cm^{-2} and then sintered in air on a Pt foil at $1100\text{ }^{\circ}\text{C}$ for 1.5 h. Optical microscopy was used to examine the polished ceramic surfaces (before and after thermal etching at $900\text{ }^{\circ}\text{C}$ for 15 min) in order to determine the porosity and grain morphology, respectively. Sintered discs were shaped to a thickness:diameter ratio of 1:10 and electrodes were painted on the major faces so as to prepare capacitor samples for electrical measurements. The samples were poled in a silicon oil bath at $200\text{ }^{\circ}\text{C}$ with fields between 50 and 95 kV cm^{-1} . Piezoelectric d_{33} coefficients were measured using a Berlincourt meter. Dielectric and elastic parameters together with electromechanical coupling factors, were measured by the resonance method, using an iterative method described elsewhere,²⁴ with a HP4192A impedance analyzer.

Results and discussion

Table 1 summarizes the milling process and annealing conditions for the different samples studied as well as the products identified. The differences in the X-ray diffraction patterns of samples milled for increasing times are compared in Fig. 1. The pattern showing the mixture of starting oxides before milling gradually broadened with increasing milling time up to 168 h, where an amorphization process was observed; after 336 h of milling time only the amorphous phase is observed.

In order to study the crystallization process of the $\text{Bi}_3\text{NbTiO}_9$ Aurivillius phase, the thermal behaviour of the amorphous phase (336 h of milling) was studied by both differential thermal analysis and X-ray powder diffraction methods. As can be observed in Fig. 2, DTA shows the existence of two irreversible exothermic processes centred at $370\text{ }^{\circ}\text{C}$ and $560\text{ }^{\circ}\text{C}$, respectively. X-Ray diffraction patterns recorded at higher temperatures (Fig. 3) confirm the formation of two well defined crystalline phases in the temperature range observed in DTA. The product remains amorphous up to $330\text{ }^{\circ}\text{C}$, whereas at $390\text{ }^{\circ}\text{C}$ it appears as a highly crystallized phase having a fluorite type structure. This correlates with the first exothermic peak observed in DTA. This phase remains unaltered up to $500\text{ }^{\circ}\text{C}$. The formation of this fluorite phase has been previously reported in the synthesis of ferroelectric Aurivillius thin films of composition $\text{Bi}_2\text{SrNb}_2\text{O}_9$ (SBN).^{25–27} These authors claim the crystallization at $650\text{ }^{\circ}\text{C}$ of a dominant

Table 1 Milling times and annealing conditions for $3\text{Bi}_2\text{O}_3:\text{Nb}_2\text{O}_5:2\text{TiO}_2$ samples and resultant products (M=mixture of phases, A=amorphous phase, P= $\text{Bi}_3\text{NbTiO}_9$ Aurivillius phase, tr=trace, lc=low crystallinity)

Annealing conditions $T/\text{ }^{\circ}\text{C}$ (t/h)	Milling time/h					
	0	3	24	72	168	336
—	M	M	M	M	A	A
500 (12)	M	M	M	M	M+P (tr)	M+P
600 (12)	M	—	—	—	P+M	P(lc)
700 (12)	M	—	—	—	P+M(tr)	P(lc)
800 (3)	—	—	—	—	P	P
800 (12)	M+P(tr)	P+M	P+M	P+M	—	—
850 (12)	M+P	P+M	P+M	P+M(tr)	—	—
900 (12)	P+M	P	P	P	—	—
1000 (12)	P+M(tr)	—	—	—	—	—
1050 (12)	P	—	—	—	—	—

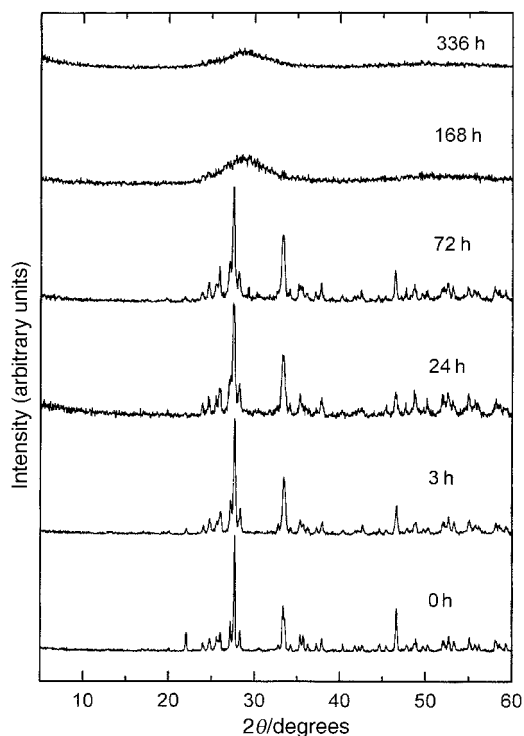


Fig. 1 X-Ray powder diffraction patterns of $3\text{Bi}_2\text{O}_3:\text{Nb}_2\text{O}_5:2\text{TiO}_2$ oxide mixture after different milling times. A mixture of starting oxides is observed up to 168 h of mechanical milling.

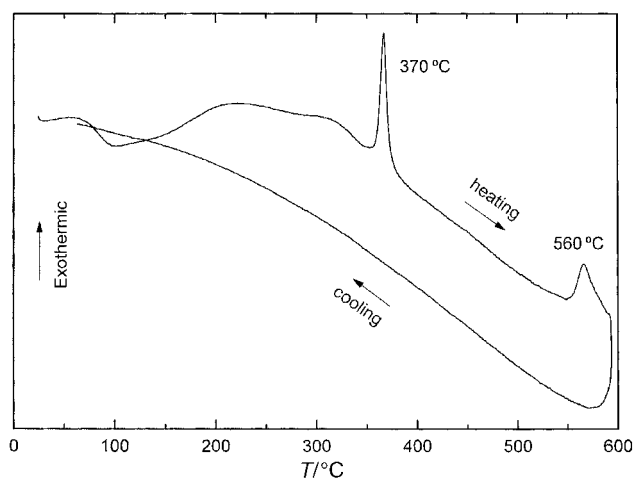


Fig. 2 Differential thermal analysis of $3\text{Bi}_2\text{O}_3:\text{Nb}_2\text{O}_5:2\text{TiO}_2$ amorphous powder (336 h of mechanical milling).

metastable fluorite phase, from thin films prepared by different deposition methods.

It is worth noting that such a fluorite phase has never been isolated as a pure phase and has not been detected in classical solid state synthesis methods. This material seems to exhibit an interesting defect fluorite-type structure with 10% of anion vacancies and showing disorder in both cationic and anionic lattices, in the same way as recently reported for the oxide Bi_3NbO_7 .²⁸ The complete structural characterization of this material, as well as its behaviour as an ionic conductor will be reported elsewhere.

After the formation of the fluorite phase Osaka *et al.*²⁷, upon studying Aurivillius thin films, considered the existence of a second transition at $750\text{ }^{\circ}\text{C}$ to give the pyrochlore phase, to be due to the presence of Bi-poor composition areas in the film, and the final formation of the Aurivillius phase after heat treatment at 775 or $800\text{ }^{\circ}\text{C}$. By contrast, in our case, the formation of a pyrochlore phase was not observed, probably

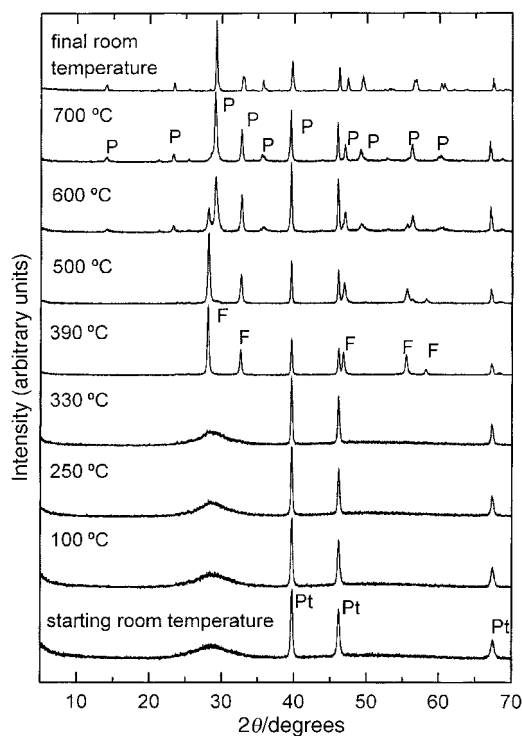


Fig. 3 X-Ray diffraction patterns at increasing temperatures of 3Bi₂O₃:Nb₂O₅:2TiO₂ amorphous powder (336 h of mechanical milling; Pt=platinum, F=fluorite phase, P=Bi₃NbTiO₉ Aurivillius phase).

owing to the very homogeneous composition of the starting amorphous product. Fig. 3 shows that crystallization of the Aurivillius phase starts at 600 °C, and that this appears mixed with a small quantity of the fluorite phase. Thus, the second exothermic effect observed in the DTA curve is attributed to the formation of the crystalline Bi₃NbTiO₉ Aurivillius phase. At 700 °C the Aurivillius oxide is isolated as a single phase with no further transformations observed during the cooling process. This represents a decrease of the reported formation temperature of such a phase¹ by some 350 °C.

We have carried out several experiments with different milling times and annealing temperatures and times, to obtain detailed information about the Aurivillius phase formation process.

For comparative purposes the oxide Bi₃NbTiO₉ was also prepared by a traditional solid state chemistry method, observing that successive thermal treatment at increasing temperatures between 500 and 1050 °C, for 12 h each, are required to isolate a pure and crystalline sample of this material. Milling times of 3, 24 and 72 h, lead only to very slight changes of starting reactants (Fig. 1), but the subsequent annealing treatments show that mechanochemical activation has already started. The changes in the X-ray diffraction patterns of reactants milled for 72 h after annealing at various temperatures for 12 h are compared in Fig. 4. In fact, in three cases (800, 850 and 900 °C) the results show only small differences (Table 1) with the presence of a mixture of starting oxides for treatment at 500 °C and the appearance of an Aurivillius phase upon annealing at 800 °C but mixed with small quantities of impurities. Only in the case of treatment at 900 °C for 12 h was it possible to obtain a pure and well crystallized Bi₃NbTiO₉ oxide.

Fig. 5 and Table 1 summarize the obtained results after annealing for the sample milled for 168 h. In this case the starting product is amorphous (Fig. 1) as is typical for powders undergoing grain size reduction.²⁹⁻³¹ The main effect of an annealing at 500 °C is the crystallization of a mixture of phases in which traces of the Aurivillius phase can be observed.

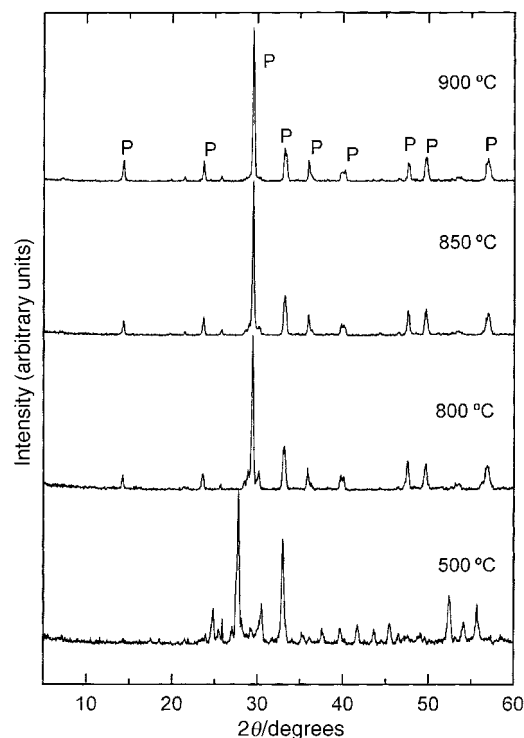


Fig. 4 X-Ray diffraction patterns of the oxide mixture milled for 72 h after annealing to various temperatures (P=Bi₃NbTiO₉ Aurivillius phase).

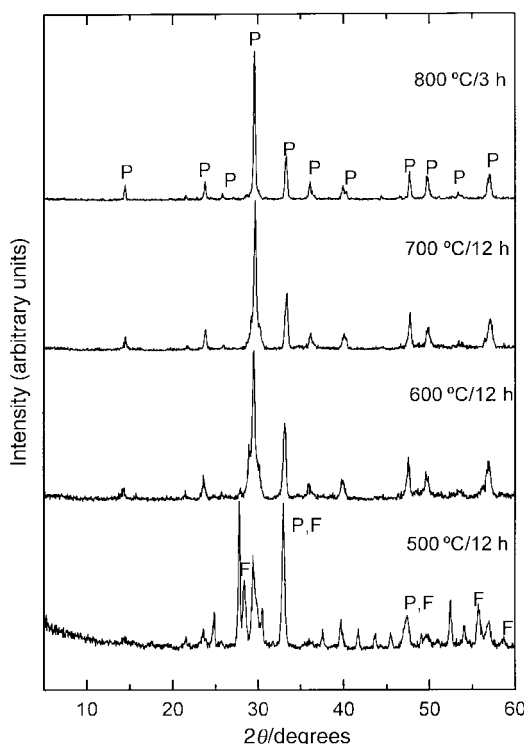


Fig. 5 Change in the X-ray diffraction patterns of the powder milled for 168 h after annealing at various temperatures (F=fluorite phase, P=Bi₃NbTiO₉ Aurivillius phase).

Annealing at 700 °C gives rise to the appearance of a poorly crystalline and, probably, impure Bi₃NbTiO₉ phase, which becomes free of secondary phases upon annealing to 800 °C for only 3 h.

When the starting product is the amorphous sample obtained by 336 h of mechanical milling, the annealing temperature to obtain a pure, although not fully crystallized,

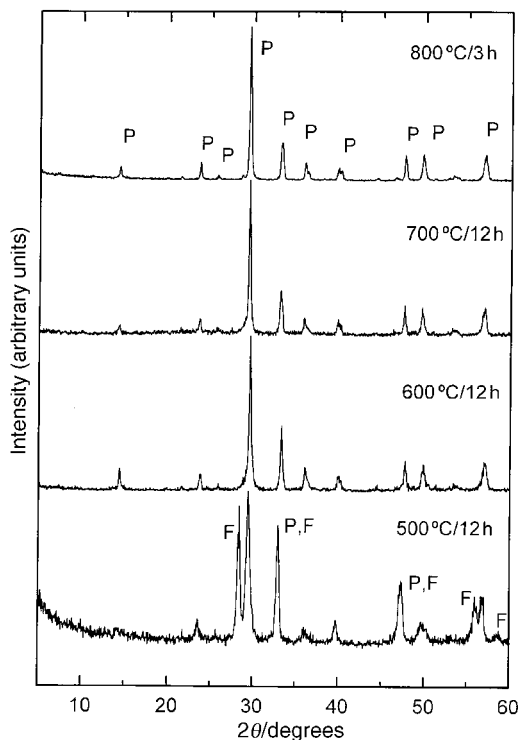


Fig. 6 Change in the X-ray diffraction patterns of the sample milled for 336 h after annealing to various temperatures (F=fluorite phase, P= $\text{Bi}_3\text{NbTiO}_9$ Aurivillius phase).

Aurivillius phase is as low as 600 °C (Fig. 6 and Table 1). Crystallization occurs upon annealing to 800 °C for 3 h. The different behaviour observed between samples obtained by 168 and 336 h of milling must be related to the degree of amorphization. The latter shows a more accentuated amorphous character, indicating a smaller grain size. In general, in polycrystalline materials fracture is most likely to occur along defects and grain boundaries in the structure. However, for longer milling time the grains become smaller (submicrometer) and less defective. Therefore, at some point of the milling process the greatest part of the defects have disappeared.¹¹ At this point the sample has stored a great amount of energy due to impacts, a prerequisite for a lower temperature synthesis of the Aurivillius phase.

The achievement of synthesis of Aurivillius phases at some 350 °C below that required when using traditional solid state routes is clearly significant.

Table 2 compares the density, dielectric, piezoelectric and elastic parameters of two ceramics prepared from powder crystallized in successive steps by thermal treatments up to 1050 °C and from amorphous powder after milling for 336 h.

Owing to the lamellar morphology of the conventionally

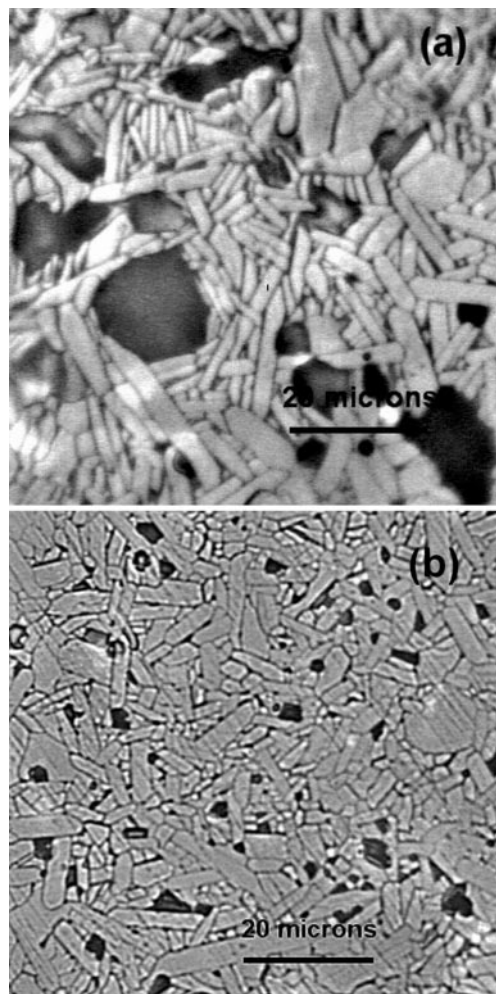


Fig. 7 Optical micrographs of polished and thermally etched surfaces of ceramics prepared (a) from conventionally crystallized powder and (b) from amorphous powder, sintered at 1100 °C for 1 h.

crystallized powder, in which the *c*-axis is perpendicular to the larger surfaces, it is difficult to obtain a high degree of packing of the grains by cold-pressing. Natural sintering gives rise to porous ceramics, low dielectric constants, low polarizability and poorly piezoelectric materials (Table 2). The alternative to sintering has previously been to use a hot-pressing procedure.³² As a result of the simultaneous application of pressure and high temperature, the lamellar grains tend to pile on top of each other with the *c*-axis parallel to the applied pressure and the hot-pressed ceramics present a texture which is not polarizable and also show anisotropic mechanical properties. These factors result in materials which are not piezoelectric.

Table 2 Dielectric, piezoelectric and elastic parameters of ceramics processed from crystallized and amorphous powders

Parameters of ceramics sintered at 1100 °C (1 h)	Ceramic from crystallized powder by steps up to 1050 °C	Ceramic from amorphous powder by milling during 336 h
Density (g cm^{-3}) and % of theoretical density (8.28g cm^{-3})	6.16 (74%)	7.65 (92%)
Dielectric permittivity (ϵ) at 1 kHz	89	120
Dielectric loss at 1 kHz ($\tan\delta$)	0.004	0.005
Maximum electric poling field applied at 200 °C (kV cm^{-1})	65	95
Piezoelectric coefficient d_{33} (pC N^{-1}) at 100 Hz	1	4
Planar electromechanical coupling factor (K_p)	0.26	1.21
Planar frequency number ($N_p/\text{kHz mm}$)	2024	2591
Elastic compliance s_{11}^E ($10^{-12} \text{m}^2 \text{N}^{-1}$)	16.7	8.5
Elastic stiffness c_{11}^E (10^{-10}N m^{-2})	6.3	12.4
Thickness electromechanical coupling factor (K_t)	Not measurable	2.43
Thickness frequency number ($N_t/\text{kHz mm}$)	Not measurable	2088

An alternative method to obtain isotropic piezoelectric ceramics is the use of an amorphous powder which gives place, directly, by natural sintering, to more dense ceramics as shown in the optical micrograph of Fig. 7. In a unique thermal process both crystallization and sintering take place. Thus, the growth of the grains generated in this thermal treatment from the amorphous powder is constrained by the surrounding grains and the generated porosity is lower than for a conventionally crystallized particle [Fig. 7(a)]. The grain growth is not oriented with the consequence of reduced porosity and higher homogeneity [Fig. 7(b)] and isotropic character. The ceramics are mechanically stiffer than those obtained from crystallized powders and, as a consequence of the lower porosity, such ceramics can support higher electric poling fields resulting in better piezoelectric coefficients (Table 2).

Conclusions

The mechanochemical activation of $3\text{Bi}_2\text{O}_3:\text{Nb}_2\text{O}_5:2\text{TiO}_2$ mixtures gives rise to progressive amorphization of the powder with increasing milling times. The subsequent annealing process allows: (i) the formation at low temperature of a fluorite-type metastable phase, which has not previously been isolated from powders obtained by classical reaction methods; (ii) an important lowering by some 350°C of the temperature at which the Aurivillius-type structure oxide $\text{Bi}_3\text{NbTiO}_9$ is obtained. Complete amorphization has been revealed as a critical feature to improve the synthesis of such phases. This can be attributed to the drastic fracture of grains and maximum energy storage, due to impacts, which leads to a reduced thermal energy required for reaction.

Ceramics prepared by natural sintering from the amorphous powder are less porous, stiffer, more polarizable and present a higher piezoelectric response than those obtained from crystallized powders.

Milling is thus proposed as an interesting alternative route for piezoelectric ceramic material processing, by favouring synthesis and sintering, particularly for materials requiring high temperatures and long reaction times.

Acknowledgements

We wish to express our gratitude to CICYT and CAM of Spain for financial support through the research projects MAT97-0711 and 07N/0061/1998, respectively.

References

- 1 B. Aurivillius, *Ark. Kemi.*, 1949, **1**, 463.
- 2 H. J. Cho, W. Jo and T. W. Noh, *Appl. Phys. Lett.*, 1994, **65**, 1525.
- 3 W. Jo, H. J. Cho, T. W. Noh, B. I. Kim, D. Y. Kim, Z. G. Khim and S. I. Kwun, *Appl. Phys. Lett.*, 1993, **63**, 2198.
- 4 W. Jo, K. H. Kim and T. W. Noh, *Appl. Phys. Lett.*, 1995, **66**, 3120.
- 5 H. S. Brooks and D. Damjanovic, *Proc. Third Euro-Ceram*, 1993, **2**, 199.
- 6 H. Watanabe, T. Kimura and T. Yamaguchi, *J. Am. Ceram. Soc.*, 1991, **74**, 139.
- 7 O. Alvarez-Fregoso, *J. Appl. Phys.*, 1997, **81**, 1387.
- 8 O. Auciello, J. F. Scott and R. Ramesh, *Phys. Today*, July, 1998.
- 9 P. Durán-Martín, A. Castro, P. Millán and B. Jiménez, *J. Mater. Res.*, 1998, **13**, 2565.
- 10 V. A. Isupov, *Inorg. Mater.*, 1997, **33**, 936.
- 11 K. Tkacova, in *Mechanical Activation of Minerals*, Elsevier, Amsterdam, 1989, pp. 1–25.
- 12 K. Hamada, T. Isobe and M. Senna, *J. Mater. Sci. Lett.*, 1996, **15**, 603.
- 13 Y. Chen, *J. Alloys Compd.*, 1998, **266**, 150.
- 14 T. Esaka, S. Takai and N. Nishimura, *Denki Kagaku*, 1996, **64**, 1013.
- 15 X. Zhou, F. Wu, B. Yin, C. Dong, J. Li, W. Zhu, S. Jia, Y. Yao and Z. Zhao, *Physica C*, 1994, **233**, 311.
- 16 J. M. Gonzalez-Calbet, J. Alonso, E. Herrero and M. Vallet-Regi, *Solid State Ionics*, 1997, **101/103**, 119.
- 17 G. S. Kodakov, *Colloid J.*, 1994, **56**, 84.
- 18 E. Kristof, A. Z. Juhasz and I. Vassanyi, *Clays Clay Miner.*, 1993, **41**, 608.
- 19 V. V. Boldyrev, *Solid State Ionics*, 1993, **63**, 537.
- 20 T. Isobe and M. Senna, *J. Solid State Chem.*, 1991, **93**, 358.
- 21 V. M. Vidojkovic, A. R. Brankovic and S. D. J. Milosevic, *Mater. Lett.*, 1997, **31**, 55.
- 22 A. R. Brankovic, V. M. Vidojkovic and S. D. J. Milosevic, *J. Solid State Chem.*, 1998, **135**, 256.
- 23 P. Butyagin, *Uspekhi Khim.*, 1994, **12**, 1031.
- 24 C. Alemany, L. Pardo, B. Jimenez, F. Carmona, J. Mendiola and A. M. Gonzalez, *J. Phys. D: Appl. Phys.*, 1994, **27**, 148.
- 25 K. Hironaka, T. Ami, C. Isobe, N. Nagel, M. Sugiyama, Y. Ikeda, K. Watanabe, A. Machida, K. Miura and M. Tanaka, *Bull. Solid-State Phys. Appl. (JSAP Div. Solid-State Phys. Appl.)*, 1995, **1**, No. 4, 15.
- 26 T. J. Boyle, C. D. Buchheit, M. A. Rodriguez, H. N. Al-Shareef, B. A. Hernandez, B. Scott and J. W. Ziller, *J. Mater. Res.*, 1996, **11**, 2274.
- 27 T. Osaka, A. Sakakibara, T. Seki, S. Ono, I. Koiwa and A. Hashimoto, *Jpn. J. Appl. Phys.*, 1998, **37**, 597.
- 28 A. Castro, E. Aguado, J. M. Rojo, P. Herrero, R. Enjalbert and J. Galy, *Mater. Res. Bull.*, 1998, **33**, 31.
- 29 T. Ikeya and M. Senna, *J. Mater. Sci.*, 1987, **22**, 2497.
- 30 T. Ikeya and M. Senna, *J. Non-Cryst. Solids*, 1988, **105**, 243.
- 31 T. Ikeya and M. Senna, *J. Non-Cryst. Solids*, 1989, **113**, 51.
- 32 P. Durán-Martín, Ph.D. Thesis, Universidad Autónoma de Madrid, Madrid, 1997.

Paper 9/02492A